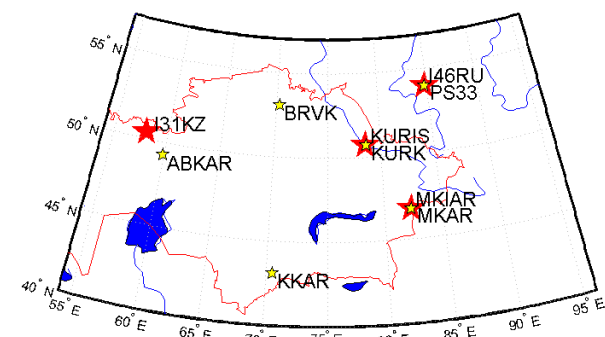


It was also shown that the other stations also detect these signals including the infrasound array I31KZ. However not only microseisms from the ocean storms but also permanently acting sources of other nature were recorded by the KKAR and MKAR seismic arrays. For example, signals from a source southward from MKAR were detected. The parameters (frequency, velocity of arrival) of the signals differ strongly from that of microseisms. There were also found the huge difference in apparent velocities explained by different types of seismic phases. Later studies found out that the source of the signals at MKAR are likely icequakes at the Inylcheck glacier, Tyan-Shan [31, 32]. Attempt to predict the location of microbarom and microseism source region was done. The prediction was based on a simplified approach assuming the source regions to be located where ocean wave height reaches its maximum value. The azimuths to those areas were found for each station using water wave heights from ECMWF [33]. Comparison of observation results and the predicted azimuth to the source region were made. Observations and predictions consistent to a first order, although some systematic azimuthal errors were noted for ABKAR.

OBSERVATION SYSTEM

The observation network of IGR, especially its infrasound part, was improved since this previous study, Figure 2. Two new infrasound arrays have been installed in Kazakhstan. These are infrasound arrays in Kurchatov [34] and in Makanchy. KNDC has also started to use the data of Russian array I46RU.



Yellow stars are seismic arrays and red stars are infrasound arrays. Russian infrasound array I46RU and seismic array PS33 are also shown as their data are actively used by KNDC. At three points both seismic and infrasound arrays are collocated. Distance between I31KZ infrasound array and ABKAR seismic array is near 200 km.

Figure 2. Arrays of the monitoring network of the IGR

Such a development suggests that a new study of microbaroms and microseisms with the data of the Kazakhstani stations will provide additional useful results. These results can also be enhanced by using more accurate method of the source prediction that is described below. Seismic arrays ABKAR, BVAR, KKAR and MKAR are similar in configuration. They consist of nine elements with aperture of about 5 km. The ABKAR array configuration is shown by Figure 3 as an example.

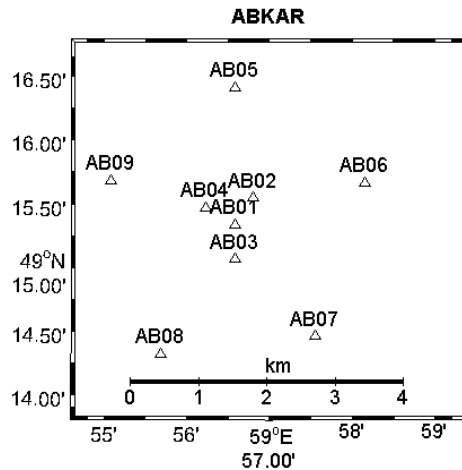


Figure 3. Configuration of the ABKAR seismic array. It consists of 9 elements with a central point, inner circle of three elements and outer circle of five elements.

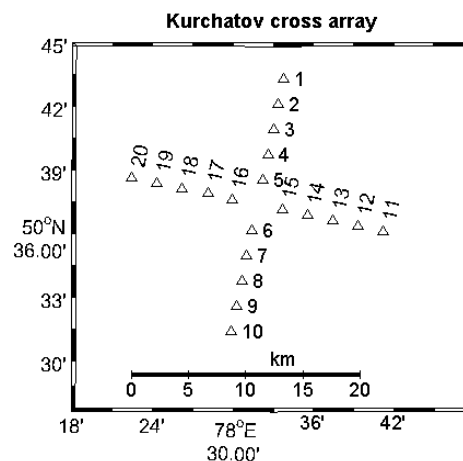


Figure 4. Configuration of the Kurchatov Cross seismic array which consists of 20 short period sensors

The Kurchatov cross array differs from the other seismic stations considering its large aperture of 22 km and the number of elements Figure 4. There are short period vertical sensors GS21 at ABKAR, BVAR, KKAR and MKAR. Kurchatov Cross consists of CMG-3V. Although the frequency band 0.1–0.3 Hz is at the edge of the frequency response of the sensors, they can record well the microseisms. Figure 5 shows the frequency response of GS-21. The frequency response of CMG-3V is similar.

MKIAR and Kurchatov are two new infrasound arrays Kurchatov is at Northeast and MKIAR at East of Kazakhstan. Their aperture is about of 1 km. MKIAR consist of 9 elements. Kurchatov has only 4. IS31 and IS46 are IMS stations. The first one is located Northwest of Kazakhstan and the second one at Altay, Russia. Their apertures are 2.1 and 2.8 km respectively [35]. The number of elements at IS31 is 8 and 4 at IS46. Microbarometers MB2000 and MB2005 are used at IS31, IS46 and Kurchatov and Chapparel Physics microbarometers are installed at MKIAR. Figure 6 shows the

frequency response of the MB2000 microbarometer. The frequency responses of other infrasound sensors used are similar to MB2000 with a flat response between 0.01 and 5.0 Hz.

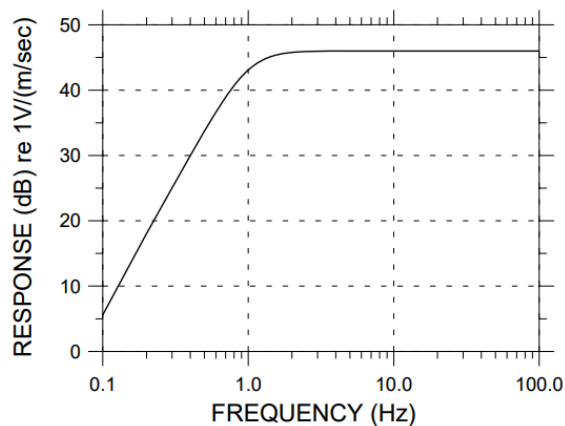


Figure 5. Frequency response of the GS-21 sensor

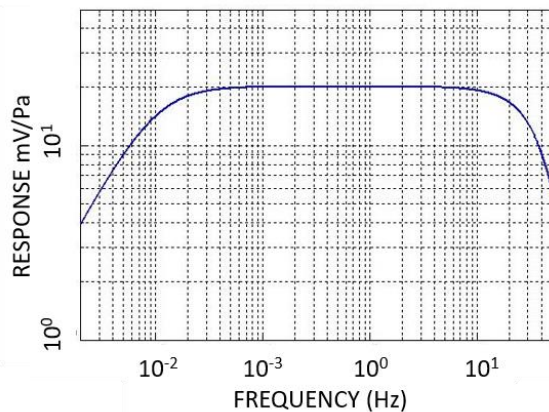


Figure 6. Frequency response of the MB2000 microbarometer

The stations in the network are part of the different global networks such as the IMS, and IRIS. KNDC has been collaborating for several years with the institutions responsible for these networks and leading seismic and infrasound centers. These are Data Center (IDC) of the Comprehensive Nuclear-Test-Ban Treaty Organization (CTBTO, Austria), Air Force Technical Applications Center (AFTAC, USA), Commissariat à l'Énergie Atomique (CEA, France) and others.

SIGNAL DETECTION: THE PMCC METHOD

Microbarom signals are detected using the PMCC method. This algorithm [30] widely used to process infrasound signals. Processing was carried out in 15 log-scaled frequency band between 0.01 and 5 Hz using a standardized configuration [36, 37]. The windows length varied from 600 s for the lowest frequency up to 30 s for the uppermost. In contrast with infrasound, processing seismic data with PMCC still needs dedicated tuning in the frequency band of interest. Thus the configuration was specially chosen for this study and

proved to be efficient for the detection of microseism signals. The data were processed in the frequency band 0.05–0.3 Hz in 10 windows of equal length of 200 s. Due to the low frequency composition of microseisms signals, processing was done with decimation. Originally seismic waveforms have sampling frequency of 40 Hz. It was checked that decimation down to 10 Hz does not affect the processing result at the frequency range 0.1–0.3 Hz and at the same time significantly reduce the computational time.

SOURCE MODELLING

The principles that were used to predict the location of the regions where microseisms and microbaroms are generating are based on classical work of Longuet – Higgins [6]. In this paper it is shown how opposing waves and their second order nonlinear interactions can generate propagating acoustic waves in the ocean which produce seismic noise by exciting the ocean floor. Hasselmann [38, 39] generalized this phenomenon to random waves and wave-wave interactions. They both show that if we consider two nearly opposing waves interacting, the resulting frequency of interest will double the frequency of water wave.

Ardhuin et al. 2011 [10] developed a numerical model based on Longuet-Higgins-Hasselmann theory for the generation of Rayleigh waves, considering an equivalent pressure source at the undisturbed surface of the ocean. Sources of microseisms are provided by IFREMER [40] – ‘p21’ – as a composite calculated from the wave-action model WaveWatchIII (WW3 – developed by the NOAA and distributed by IFREMER).

These nonlinear interactions also generate waves propagating in the atmosphere – known as microbaroms. As the source term at the ocean surface is the same as for microseisms – only the amplitude might change due to a resonance term in finite depth ocean [7, 8], the same ‘p21’ model was used to make qualitative comparisons with observations. Figure 7 shows example of the source power distribution. The source intensity was calculated on February 2, 2017 in the 0.1–0.3 Hz frequency range. Sources in white areas were not taken into account as the probability to get signals from these regions at that time of the year in Kazakhstan is rather small considering both source intensity and propagation range.

COMPARISON OF THE OBSERVATIONS AND PREDICTIONS

Long term microbarom observations for the Central Eurasia area were kindly provided by CEA. These contains four years of the PMCC detection results at IS31 (Figure 8) and IS46 (Figure 9) in a frequency range 0.01–4 Hz. Only detections in the 0.1–0.3 Hz band were selected. Azimuths to the predicted source regions are shown by black circles.

**SIGNALS FROM SEVERE OCEAN STORMS IN NORTH ATLANTIC
AS IT DETECTED IN KAZAKHSTAN: OBSERVATION AND MODELLING**

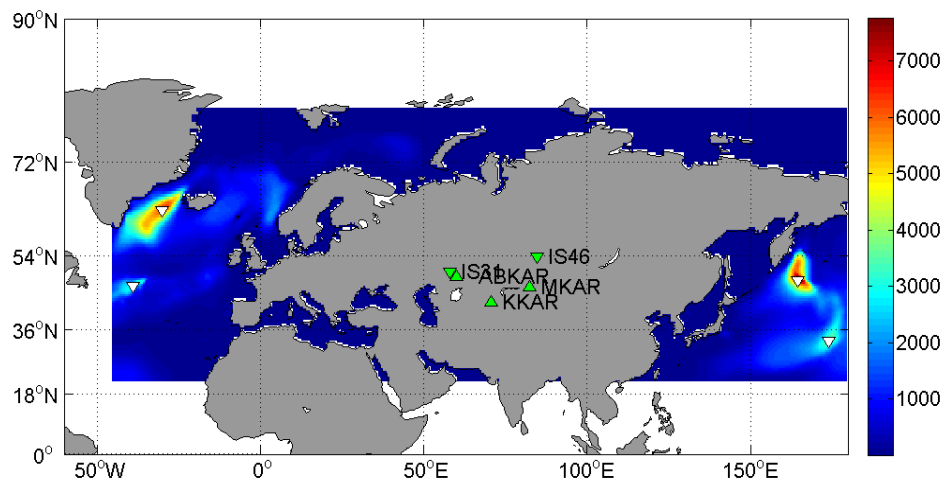
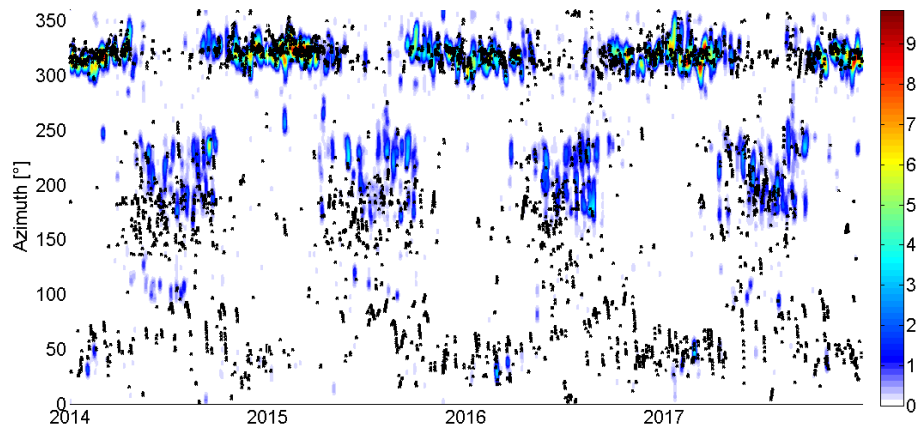
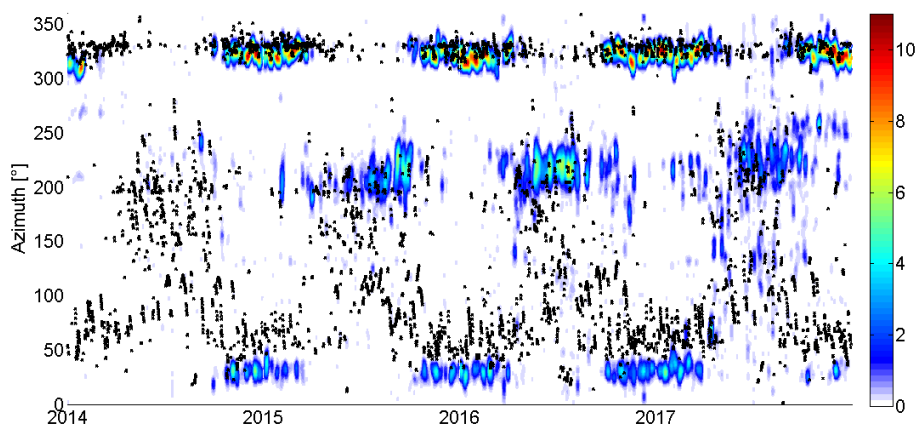


Figure 7. Example of the source energy distribution. The map shows the energy distribution averaged for the entire day of February 2, 2017 in the frequency range 0.1–0.3 Hz. Data about the ocean wave energy are provided by the IFREMER [10].



Black circles are the predicted back-azimuths. The colorbar codes the logarithm of the number of detections.

Figure 8. Four years of the PMCC detections at IS31 in the frequency range 0.1–0.3 Hz (the PMCC bulletins are kindly provided by CEA)



Black circles are the predicted back-azimuths to source. The colorbar codes the logarithm of the number of detections.

Figure 9. Four years of the PMCC detections at IS46 in the frequency range 0.1–0.3 Hz (the PMCC bulletins are kindly provided by CEA)

For both IS31 and IS46 there is a good match between observations and modelling results in range 300° – 350° that corresponds to signals originating from North Atlantic. There are predictions of signals from the South with poor correlation with observations. There are also predictions of signals from North Pacific. At IS46 there are corresponding observations which are shifted in azimuth by approximately 25° . All these results show that it is needed to take into account for the atmospheric effects on long range propagation. The lack of detections to North Pacific at IS31 also suggests that it is needed to incorporate wind effects on the wave attenuation.

The comparisons of microseism observations and simulation results during two-month period show similar pictures when using seismic data. Figure 10–13 show observations and simulations at ABKAR, KKAR, MKAR and Kurchatov cross respectively.

Figure 11 PMCC detections and source region simulation for KKAR seismic array. Color represents the apparent velocity of the detected microseisms. Black crosses indicate direction to the main and local maxima of the energy in the simulated source regions.

There is a good consistency between observations and modelling results at all stations. Despite of some systematic errors there are stable records of North Atlantic microbaroms. Mean apparent velocity of microbarom detections is close to 7 km/s. However, at some time intervals, apparent velocity rises up to 16 km/s. At the same periods, back-azimuths vary up to 80° , Figure 14. This effect is not observed at ABKAR, small at KKAR and large at MKAR and at Kurchatov Cross arrays. Some systematic offset between the observed and predicted back-azimuths appear at all stations. This offset is approximately 10° – 20° clockwise for observations at ABKAR and KKAR and almost the same range but counter clockwise at Kurchatov Cross and MKAR.

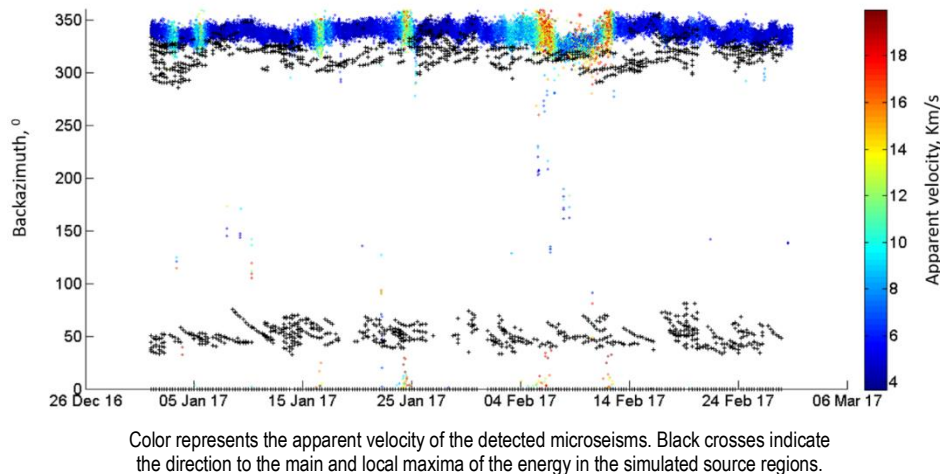


Figure 10. PMCC detections and source region simulation for ABKAR seismic array

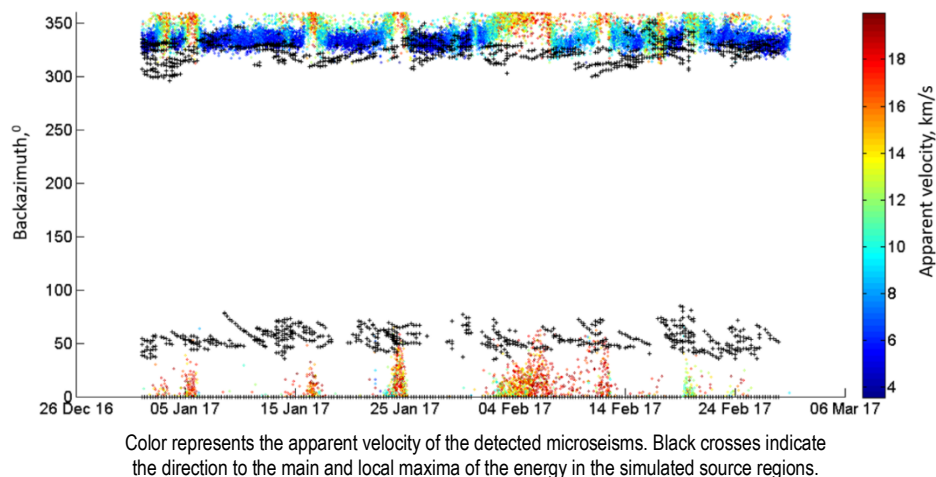
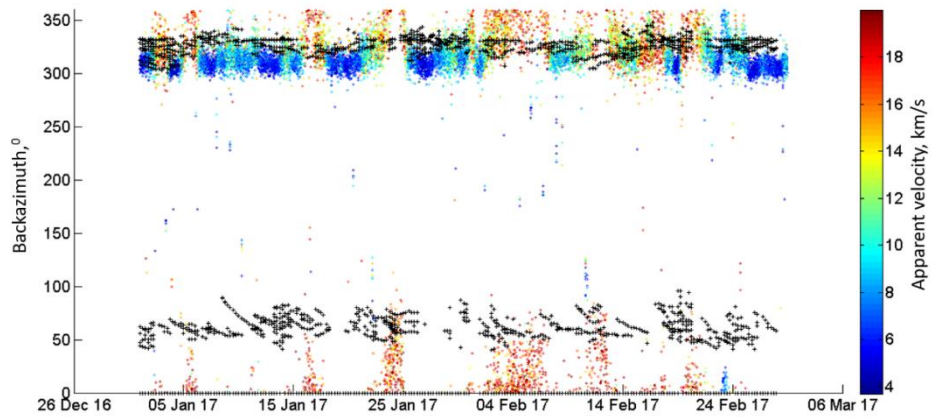


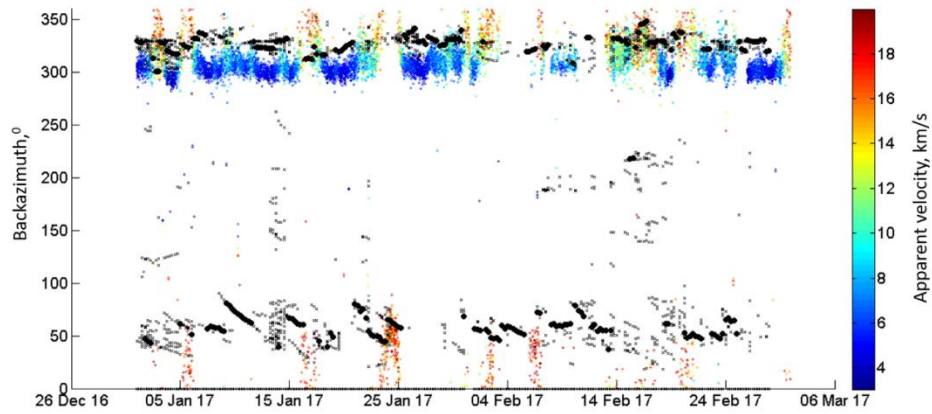
Figure 11. PMCC detections and source region simulation for KKAR seismic array

SIGNALS FROM SEVERE OCEAN STORMS IN NORTH ATLANTIC
AS IT DETECTED IN KAZAKHSTAN: OBSERVATION AND MODELLING



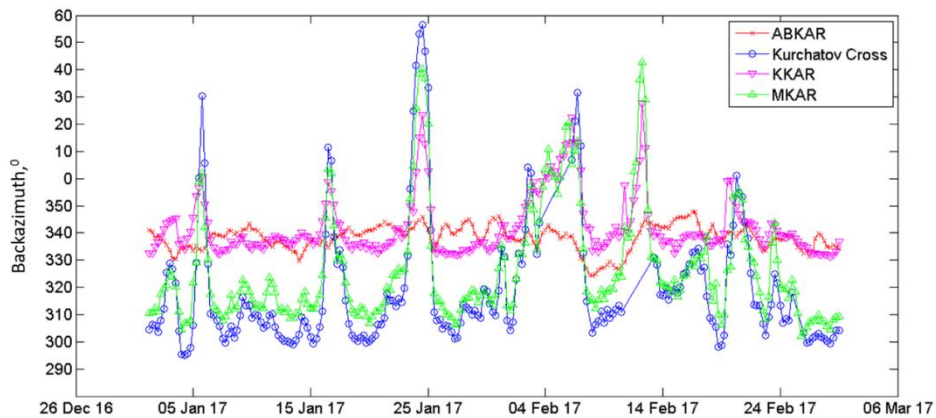
Color represents the apparent velocity of the detected microseisms. Black crosses indicate the direction to the main and local maxima of the energy in the simulated source regions.

Figure 12. PMCC detections and source region simulation for MKAR seismic array



Color represents the apparent velocity of the detected microseisms. Black circles indicate the direction to the main maxima of the energy in the simulated source regions, black crosses point to the local maxima.

Figure 13. PMCC detections and source region simulation for Kurchatov-Cross seismic array

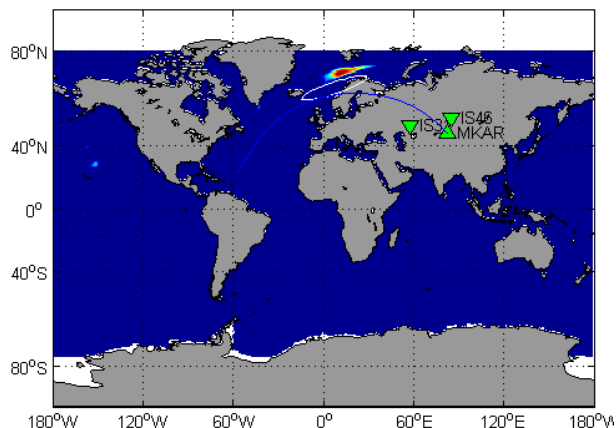


Each point represents an averaged value of the measures over a 6 h time window

Figure 14. Comparison of the observed back-azimuths at four seismic arrays. Detections correspond to the period between January and February 2017.

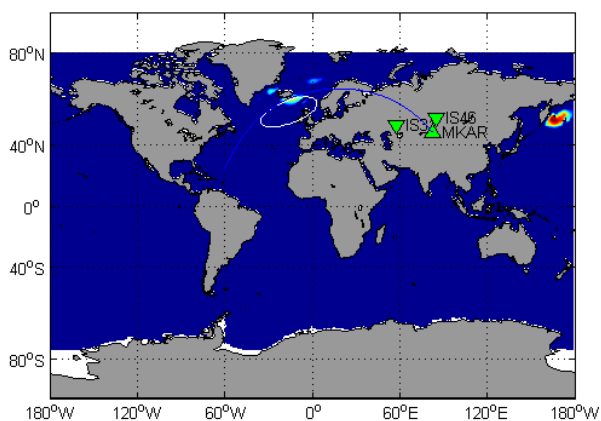
LOCALIZATION OF THE SOURCE REGION

As microbaroms and microseisms are recorded by the network, it is possible to localize the source region. Figure 15 shows first approach of such localization.



White line represents the 90% error ellipse for the locations determined using cross bearing with detections at IS31 and IS46. The blue line indicates the backazimuth calculated from MKAR.

Figure 15. Localization of the microbaroms source regions averaged in January 2017. The map shows the simulation results of microbarom intensity.



White line represents the 90% error ellipse for the locations determined using cross bearing with detections at IS31 and IS46. The blue line indicates the backazimuth calculated from MKAR.

Figure 16. Localization of the microbaroms source regions averaged in February 2017. The map shows the simulation results of microbarom intensity.

Cross-bearing locations use detections at IS31 and IS46. The bearings were averaged for each 6 hours of observations. Error ellipse of the solutions is compared with the intensity distribution of the source region, shown in color on the Figure 15. The signal attenuation calculated for effective point placed in between IS31 and IS46 was taken into account when the source

strength was calculated. A simplified formulation of the semi-empirical attenuation relation considering only the combined effects of geometrical spreading and absorption was used [41] (1):

$$Ap(f, V_{eff-ratio}) = \frac{1}{R} 10^{\frac{\alpha(f)R}{20}} + \frac{R^{\beta(f, V_{eff-ratio})}}{1 + 10^{\delta(f)}}, \quad (1)$$

$$A = R^{(-0.95)}. \quad (2)$$

These results shows first order agreement between observations and modelling results in the North Atlantic region, although some systematic errors are visible. These errors could likely be reduced by accounting for atmospheric effects on long-range infrasound propagation.

CONCLUSIONS

Historical records of the Kazakhstani network have been collected and processed to characterize microseism and microbarom permanently recorded. The existing seismo-acoustic network with collocated stations offers a good opportunity to better understand coupling mechanisms at the ocean-earth-atmosphere interfaces considering the same source. Parameters for the processing using PMCC were tuned to better characterize microseisms and microbaroms. State of the art source simulation method was also chosen. The source area was localized following a cross bearing approach. Comparisons between the localization results and the predicted source regions with the maximum intensity shows satisfactory results over North Atlantic. However, there is systematic error that will hopefully be corrected considering propagation simulations. Comparisons between the observed bearings of seismic data and the source location show systematic errors which vary from one station to another. There are anomalous measured backazimuth deviations up to 80° at several intervals of time, at least at three seismic stations. Detections during these time intervals exhibit large azimuthal deviations and high apparent velocity values (15–19 km/s). The effect appears when using both small and middle aperture seismic arrays 5 and 22 km respectively. The lack of resolution of the seismic arrays due to their small aperture might contributes to these discrepancies. Array size smaller than the wavelength of the seismic signals (several tens of km for body waves) could explain an increase of the azimuthal errors. Also, it was shown in [42] that the azimuth to source measured by Kazakhstani arrays may deviate significantly from the true azimuth to source epicenter due to refraction at Kazakhstan orocline. Presence of relation between this fact and the anomalous azimuth deviations found at this study is issue for future investigations.

REFERENCES

1. Смирнов, А. А. Объяснение природы источников когерентных низкочастотных сигналов, регистрируемых мониторинговой сетью НЯЦ РК / А. А. Смирнов, В. Дубровин, Л. Эверс // Вестник НЯЦ РК, 2010. – Вып. 3. – 76–81.
2. Donn, W.L. Sea wave origin of microbaroms and microseisms / W.L. Donn, B. Naini // *J. Geophys. Res.* 1973. – V. 78. – P. 4482–4488.
3. Rind, D. Microseisms at Palisades. III—microseisms and microbaroms / D. Rind // *J. Geophys. Res.*, 1980. – 85. – P. 4854–4862.
4. Hedlin, M.A.H. Listening to the secret sounds of Earth's atmosphere / M.A.H. Hedlin, M. Garces, H. Bass, C. Hayward, G. Herrin, J. V. Olson, C. Wilson // *EOS, Trans. Am. Geophys. Un.*, 2002. – 83 (48). – P. 564–565.
5. Bowman, J.R. Ambient infrasound noise / J.R. Bowman, G.E. Baker, M. Bahavar // *Geophys. Res. Lett.*, 2005. – 32. – 09803, doi:10.1029/2005GL022486.
6. Longuet-Higgins, M.S. A theory of the origin of microseisms / M.S. Longuet-Higgins // *R. Soc. Lond. Phil. Trans.*, 1950. – A, 243. – P. 1–35.
7. Waxler, R. The radiation of atmospheric microbaroms by ocean waves / R. Waxler, E.K. Gilbert // *J. acoust. Soc. Am.*, 2006. – 119. – P. 2651–2664.
8. Arduin, F. Noise generation in the solid Earth, oceans and atmosphere, from nonlinear interacting surface gravity waves in finite depth / F. Arduin, T.H.C. Herbers // *J. Fluid Mech.*, 2013. – 716. – P. 316–348.
9. Kedar, S. The origin of deep ocean microseisms in the North Atlantic Ocean / S. Kedar, M. Longuet-Higgins, F. Webb, N. Graham, R. Clayton, C. Jones // *R. Soc. Lond. Proc.*, 2008. – A, 464. – P. 777–793.
10. Arduin, F., Ocean wave sources of seismic noise / F. Arduin, E. Stutzmann, M. Schimmel, A. Mangeney // *J. Geophys. Res. (Oceans)*, 2011. – P. 116. – 9004. – doi:10.1029/2011JC006952.
11. Stehly, L. A study of the seismic noise from its long-range correlation properties / L. Stehly, M. Campillo, N.M. Shapiro // *J. Geophys. Res.: Solid Earth.*, 2006. – 111 – 10306. – doi:10.1029/2005JB004237.
12. Stutzmann, E. Global climate imprint on seismic noise / E. Stutzmann, M. Schimmel, G. Patau, A. Maggi, // *Geochem. Geophys. Geosyst.*, 2009. – 10. – 11004. – doi:10.1029/2009GC002619.
13. Land`es, M. Origin of deep ocean microseisms by using teleseismic body waves / M. Land`es, F. Hubans, N.M. Shapiro, A. Paul, M. Campillo // *J. Geophys. Res.: Solid Earth*, 2010. – 115. – doi:10.1029/2009JB006918.
14. Hillers, G. Global oceanic microseism sources as seen by seismic arrays and predicted by wave action models / G. Hillers, N. Graham, M. Campillo, S. Kedar, M. Land`es, N. Shapiro // *Geochem., Geophys., Geosyst.*, 2012. – 13. – 1021. – doi:10.1029/2011GC003875.
15. Drob, D.P. Global morphology of infrasound propagation / D.P. Drob, J.M. Picone, M. Garc`es // *J. Geophys. Res. (Atmospheres)*, 2003. – 108. – 4680, doi:10.1029/2002JD003307.
16. Garc`es, M., Willis, M., Hetzer, C., Le Pichon, A. & Drob, D. On using ocean swells for continuous infrasonic measurements of winds and temperature in the lower, middle, and upper atmosphere / M. Garc`es, M. Willis, C. Hetzer, A. Le Pichon, D. Drob // *Geophys. Res. Lett.*, 2004. – 31. – doi:10.1029/2004GL020696.
17. Le Pichon, A. On using infrasonic from interacting ocean swells for global continuous measurements of winds and temperature in the stratosphere / A. Le Pichon, L. Ceranna, M. Garc`es, D. Drob, C. Millet // *J. Geophys. Res. (Atmospheres)*, 2006. – 111. – doi:10.1029/2005JD006690.
18. Brachet, N., Brown, D., Le Bras, R., Cansi, Y., Mialle, P. & Coyne, J. Monitoring the Earth's atmosphere with the global IMS infrasound network / N. Brachet, D. Brown, R. Le Bras, Y. Cansi, P. Mialle, J. Coyne // *Infrasound Monitoring for Atmospheric Studies*, 2010. – P. 77–118, eds Le Pichon, A., Blanc, E. Hauchecorne, A. – Springer.
19. Campillo, M. Correlations of Seismic Ambient Noise to Image and to Monitor the Solid Earth / M. Campillo, P. Roux, N. M. Shapiro // Springer. – 2011.
20. Campillo, M. New developments on imaging and monitoring with seismic noise / M. Campillo, H. Sato, N.M. Shapiro, R.D. van der Hilst // *C. R. Geoscience*, 2011. – 343. – P. 487–495.
21. Shapiro, N.M. 2005. High resolution surface-wave tomography from ambient seismic noise / N.M. Shapiro, M. Campillo, L. Stehly, M.H. Ritzwoller // *Science*, 2005. – 307. – P. 1615–1618.
22. Ritzwoller, M.H. Ambient noise tomography with a large seismic array / M.H. Ritzwoller, F.-C. Lin, W. Shen // *Comp. Rend. Geosci.*, 2011. – 343(8). – P. 558–570.
23. Mordret, A. Near-surface study at the valhall oil field from ambient noise surface wave tomography / A. Mordret, M. Land`es, N.M. Shapiro, S.C. Singh, P. Roux, O.I. Barkved // *Geophys. J. Int.*, 2013. – 193(3) – P. 1627–1643.
24. Brenguier, F. Postseismic relaxation along the San Andreas fault at Parkfield from continuous seismological observations / F. Brenguier, M. Campillo, C. Hadziioannou, N.M. Shapiro, R.M. Nadeau, E. Larose // *Science*, 2008. – 321(5895). – P. 1478–1481.
25. Brenguier, F. Towards forecasting volcanic eruptions using seismic noise / F. Brenguier, N.M. Shapiro, M. Campillo, V. Ferrazzini, Z. Duputel, O. Coutant, A. Necessian // *Nat. Geosci.*, 2008. – 1(2). – P. 126–130.
26. Hedlin, M.A.H. Infrasound: connecting the solid Earth, oceans, and atmosphere / M.A.H. Hedlin, K. Walker, D.P. Drob, C.D. de Groot-Hedlin // *Ann. Rev. Earth planet. Sci.*, 2012. – 40. – P. 327–354.
27. Evers, L.G. Listening to sounds from an exploding meteor and oceanic waves / L.G. Evers, H.W. Haak // *Geophys. Res. Lett.*, 2001. – 28. – P. 41–44.
28. Stevens, J.L. Constraints on infrasound scaling and attenuation relations from soviet explosion data / J.L. Stevens, I.I. Divnov, D.A. Adams, J.R. Murphy, V.N. Burchik // *Pure appl. Geophys.*, 2002. – 159. – P. 1045–1062.
29. Smirnov A.A. Explanation of the nature of coherent low-frequency signal sources recorded by monitoring station network of the NNC RK / A.A. Smirnov, V.I. Dubrovин, L.G. Evers, S. Gibbons // *CTBTO Science and Technology* 2011. – Vienna, Austria.

30. Cansi, Y. An automatic seismic event processing for detection and location: the P.M.C.C. method / Y. Cansi // Geophys. Res. Lett., 1995 – 22. – P. 1021–1024.
31. Михайлова, Н.Н. Ледниковые землетрясения Центрального Тянь-Шаня / Н.Н. Михайлова, И.И. Комаров / Вестник НЯЦ РК, 2009. – Вып. 3. – С. 120–126.
32. Полешко, Н.Н. Механизмы очагов землетрясений в зоне ледникового Центрального Тянь-Шаня / Н.Н. Полешко, Н.Н. Михайлова // Вестник НЯЦ РК, 2012. – Вып. 1. – С. 61–67.
33. Website ECMWF: <https://www.ecmwf.int/>
34. Беляшов, А.В. Новая инфразвуковая группа «Курчатов» / А.В. Беляшов, В.И. Донцов, В.И. Дубровин, В.Г. Кунаков, А.А. Смирнов // Вестник НЯЦ РК, 2013. – Вып. 2. – С. 24–30.
35. Edwards, W. Effect of interarray elevation differences on infrasound beamforming / W. Edwards, N. Green // Geophys. J. Int., 2012. – 190(1). – P. 335–346.
36. Le Pichon, A. Recent Enhancements of the PMCC Infrasound Signal Detector / A. Le Pichon, R.S.N.B. Matoza, Y. Cansi // Inframatics, 2010. – 26. – P. 5–8.
37. Matoza, R.S., Coherent ambient infrasound recorded by the International Monitoring System / R.S. Matoza, M. Land'es, A. Le Pichon, L. Ceranna, D. Brown // Geophys. Res. Lett., 2013. – 40. – P. 429–433.
38. Hasselmann, K. A statistical analysis of the generation of microseisms / K. Hasselmann // Rev. Geophys., 1963. – 1. – 177–210.
39. Hasselmann, K. Feynman diagrams and interaction rules of wave-wave scattering processes / K. Hasselmann // Rev. Geophys., 1966. – 4(1). – P. 1–32.
40. IFREMER Website: WW3 data <ftp://ftp.ifremer.fr/ifremer/ww3/HINDCAST/GLOBAL/> .
41. Le Pichon, A., Ceranna, L. & Vergoz, J. Incorporating numerical modeling into estimates of the detection capability of the IMS infrasound network / A. Le Pichon, L. Ceranna, J. Vergoz // J. Geophys. Res. (Atmospheres), 2012. – 117. – 5121. - doi:10.1029/2011JD016670.
42. Labonne, C. Detailed analysis of the far-regional seismic coda in Kazakhstan using array processing / C. Labonne, O. Sèbe, A. Smirnov, S. Gaffet, Y. Cansi, N. Mikhailova // Bulletin of the Seismological Society of America, 2017. – 107(2), - P. 611–623. – doi:10.1785/0120160015.

ҚАЗАҚСТАНДЫҚ ЖЕЛІСІНІҢ ДЕРЕКТЕРІ БОЙЫНША СОЛТҮСТІК АТЛАНТИКАДАҒЫ ҚАТТЫ ДАУЫЛДАРДАН СИГНАЛДАР: БАҚЫЛАУ НӘТИЖЕЛЕРІ МЕН МОДЕЛЬДЕУ

¹⁾ Смирнов А.А., ^{2,3)} Де Карло М., ³⁾ Ле Пишон А., ⁴⁾ Шапиро Н.М.

¹⁾ Қазақстан Республикасы Энергетика министрлігінің
Геофизикалық зерттеулер институты, Курчатов, Қазақстан

²⁾ Батыс Бретан Университеті (UBO), Брест, Франция

³⁾ Атом энергиясы жөніндегі комиссариаты (CEA/DAM/DIF), Арпажон, Франция

⁴⁾ Париждің Жер физикасы институты (IPGP), Париж, Франция

Мониторингтің қазақстандық желісі төрт сейсмикалық және үш инфрадыбыстық топтарынан тұрады. Топтардың жазбаларында сол-түстік шығыстан келген көптеген сигналдар табылған. Қазақстан аумағы үшін микробаромдар мен микросейсмдердің басым көзі Солтүстік Атлантика болып табылады [1]. Микросейсмдер мен микробаромдар өндірілу орындардың орналасуын өзгертуін модельдеуі теңіз толқындардың энергиясы мен қозғалысының бағыттары туралы деректердің негізінде жүргізілген. Модельдеу мен қазақстандық мониторингтік желісінің бақылауларының нәтижелерін салыстыруы жүргізілген.

СИГНАЛЫ ОТ СИЛЬНЫХ ШТОРМОВ В СЕВЕРНОЙ АТЛАНТИКЕ ПО ДАННЫМ КАЗАХСТАНСКОЙ СЕТИ: РЕЗУЛЬТАТЫ НАБЛЮДЕНИЯ И МОДЕЛИРОВАНИЕ

¹⁾ Смирнов А.А., ^{2,3)} Де Карло М., ³⁾ Ле Пишон А., ⁴⁾ Шапиро Н.М.

¹⁾ Институт геофизических исследований Министерства энергетики
Республики Казахстан, Курчатов, Казахстан

²⁾ Университет Западной Бретани (UBO), Брест, Франция

³⁾ Комиссариат по атомной энергии (CEA/DAM/DIF), Арпажон, Франция

⁴⁾ Парижский институт физики Земли (IPGP), Париж, Франция

Казахстанская сеть мониторинга состоит из четырёх сейсмических и трёх инфразвуковых групп. В записях групп найдено множество сигналов, пришедших с северо-востока. Преобладающим источником микробаром и микросейсм для территории Казахстана является Северная Атлантика [1]. Моделирование изменений положения мест генерации микросейсм и микробаром было произведено на основе данных об энергии и направлении движения морских волн. Произведено сравнение результатов моделирования и наблюдения казахской мониторинговой сети.